Loops and Strings in a Superconducting Lattice Gauge Simulator

G. K. Brennen,[1] G. Pupillo,[2] E. Rico,[3,4] T. M. Stace,[5] and D. Vodola[2]
[1]Centre for Engineered Quantum Systems, Department of Physics and Astronomy, Macquarie University, Sydney, NSW 2109, Australia
[2]icFRC, IPCMS (UMR 7504) and ISIS (UMR 7006), Universite de Strasbourg and CNRS,67000 Strasbourg, France
[3]Department of Physical Chemistry, University of the Basque Country UPV/EHU, Apartado 644, E-48080 Bilbao, Spain
[4]IKERBASQUE, Basque Foundation for Science, Maria Diaz de Haro 3, E-48013 Bilbao, Spain
[5]Center for Engineered Quantum Systems, School of Mathematics and Physics, The University of Queensland, St Lucia, Queensland 4072, Australia
(Received 12 January 2016; published 7 December 2016)

We propose an architecture for an analog quantum simulator of electromagnetism in $2+1$ dimensions, based on an array of superconducting fluxonium devices. The encoding is in the integer (spin-1) representation of the quantum link model formulation of compact $U(1)$ lattice gauge theory. We show how to engineer Gauss' law via an ancilla mediated gadget construction, and how to tune between the strongly coupled and intermediately coupled regimes. The witnesses to the existence of the predicted confining phase of the model are provided by nonlocal order parameters from Wilson loops and disorder parameters from 't Hooft strings. We show how to construct such operators in this model and how to measure them nondestructively via dispersive coupling of the fluxonium islands to a microwave cavity mode. Numerical evidence is found for the existence of the confined phase in the ground state of the simulation Hamiltonian on a ladder geometry.

DOI: 10.1103/PhysRevLett.117.240504

Gauge theories play a fundamental role in modern physics, including quantum electrodynamics and quantum chromodynamics. The discretized version of gauge theory, lattice gauge theory (LGT), is key to understanding physics ranging from quantum spin liquids to quark-gluon plasmas [1–3]. A fundamental phenomenon in gauge theories is the notion of confinement, which manifests in the absence of isolated, color-charged particles in nature; i.e., the only "physical" states are those that transform "trivially" under a gauge transformation. Yet, quantum phases of gauge field theories cannot be characterized by local order parameters. Instead, nonlocal order parameters such as Wilson loops [1] and 't Hooft strings [4] have been introduced to indicate the presence or absence of a confined phase.

Quantum link models (QLMs) provide a formulation of LGTs, in which finite-dimensional subsystems associated with edges of the lattice encode the gauge field [5–7]. Related $U(1)$ gauge models are important for understanding various condensed matter systems, including quantum spin ice models or quantum dimer models, which may exhibit deconfined critical points at $T=0$ [8]. In principle, QLMs break Lorentz invariance while relativistic $U(1)$ gauge theories in $2+1$ dimensions are always in a confinement phase at $T=0$ but may undergo a phase transition at $T_c>0$ to a deconfined phase [9]. In either case, confinement physics is a key to understanding the phenomenology.

Numerical simulation of LGTs can be computationally costly due to the size of the Hilbert space or the sign problem with quantum Monte Carlo techniques [10] (for recent proposals using tensor networks see Refs. [11–23]). An alternative approach is to build analog quantum simulators to replicate the equilibrium and dynamical properties of a system of interest. Indeed, this is one of the motivations for quantum technologies based on atomic [24–40] and superconducting platforms [41–44]. A way to measure space-time Wilson loops in atomic lattice gauge simulators (assuming localized excitations) was given in Ref. [32] but a critical outstanding problem has been the reliable measurement of nonlocal, space-like Wilson loops and 't Hooft strings.

Here, we propose an analog simulator of a pure compact $U(1)$ QLM in $2+1$ dimensions [45], based on superconducting fluxonium [46] devices placed on a square lattice. The devices operate in a finite-dimensional manifold of low-lying eigenstates, to represent "discrete" electric fluxes on the lattice. By engineering local couplings between devices, we show how to replicate the local interactions and constraints of the QLM. The couplings can be tuned to access different phases of the quantum phase diagram of the model. We demonstrate how to measure nonlocal, space-like Wilson loops and 't Hooft strings in the proposed architecture. Moreover, we report density-matrix renormalization group (DMRG) calculations of a 't Hooft disorder parameter in a QLM, and show that the QLM indeed captures confinement physics.

Quantum link model.—In the pure gauge $U(1)$ QLM, electric fluxes $\hat{E}_{\alpha,\beta}$ are defined on the links $\langle\alpha,\beta\rangle$ of a square lattice with local link state space $\mathbb{C}^{N+1}$ [circles in Fig. 1(a)]. In the electric basis, the Hilbert space is labeled by the electric fluxes on the links, $\hat{E}_{\alpha,\beta}|E_{\alpha,\beta}\rangle = E_{\alpha,\beta}|E_{\alpha,\beta}\rangle$. For a compact $U(1)$ gauge group, fluxes take integer or half integer values, $-(N/2) \le E_{\alpha,\beta} \le (N/2)$, $N \in \mathbb{Z}^+$. The local link electric-displacement operator $\hat{U}_{\alpha,\beta}$ satisfies the commutation

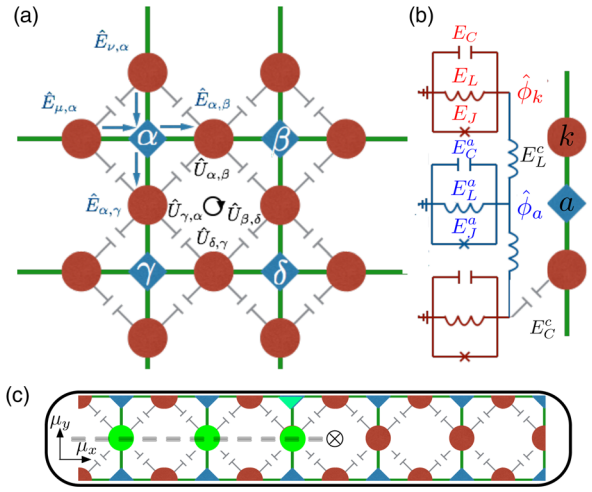

FIG. 1. $U(1)$ quantum link model engineered in a fluxonium array. (a) "Electric" $\hat{E}_{\alpha,\beta}$, and "magnetic" $\hat{U}_{\alpha,\beta}$, degrees of freedom are associated with links $\langle\alpha,\beta\rangle$ of a square lattice. The link degrees of freedom (red circles) are encoded in eigenstates of the fluxonia. The ancillae (blue diamonds) on vertices are inductively coupled to neighboring link islands to mediate the Gauss constraint and plaquette interactions are obtained via link nearest neighbor capacitive coupling. (b) Superconducting circuit elements used to build and couple components of the simulation. The link devices have local phase $\hat{\phi}_{\text{link}}$ and capacitive, inductive, and flux-biased Josephson energies E_C, E_L, and E_J, respectively, and similarly for the ancilla devices. The capacitive and inductive coupling energies are E_C^c and E_L^c. (c) A minimal quasi-1D "ladder" implementation embedded in a microwave cavity (black box), in which a 't Hooft string of link fluxonia (green circles) can be measured via an ancilla coupled to the cavity (green triangle).

relation $[\hat{E}_{\alpha,\beta}, \hat{U}_{\alpha,\beta}] = -\hat{U}_{\alpha,\beta}$ [for a detailed description see the Supplemental Material [47] (Sec. I)]. In the charge-free sector, the net electric flux at a given vertex is zero; hence, there is a conserved quantity $\hat{G}_\alpha = \hat{E}_{\mu,\alpha} + \hat{E}_{\nu,\alpha} - \hat{E}_{\alpha,\beta} - \hat{E}_{\alpha,\gamma}$. The phase of the operators can be changed locally with the $U(1)$ gauge transformation $e^{i\theta_\alpha \hat{G}_\alpha}$ and the dynamics remain invariant. The gauge invariant subspace satisfies $\hat{G}_\alpha|\text{phys}\rangle = 0$, which is the discretized Gauss law $\vec{\nabla}\cdot\vec{E}|_{\text{phys}} = 0$. In a pure gauge model, there are two competing terms in the Hamiltonian: the electric term penalizes electric flux on each link $\langle\alpha,\beta\rangle$ and the magnetic term penalizes magnetic flux on each plaquette $\square$,

$$\hat{H}_{\text{QLM}} = g_{\text{elec}}^2 \sum_{\langle\alpha,\beta\rangle} \hat{E}_{\alpha,\beta}{}^2 - \frac{1}{g_{\text{mag}}^2} \sum_{\square} (\hat{U}_{\alpha,\beta}\hat{U}_{\beta,\delta}\hat{U}_{\delta,\gamma}\hat{U}_{\gamma,\alpha} + \text{H.c.}), \tag{1}$$

where g_{elec}^2 and g_{mag}^2 are the coupling constants for the electric term and magnetic term, respectively.

We characterize the confinement of electric charges, which locally violate Gauss' law, using Wilson loops. The smallest Wilson loop operator is defined on a plaquette, $\mathcal{W} = \hat{U}_{\alpha,\beta}\hat{U}_{\beta,\delta}\hat{U}_{\delta,\gamma}\hat{U}_{\gamma,\alpha}$. This is a discrete approximation to $e^{i\oint \mathbf{A}\cdot\mathbf{dl}}$ where $\mathbf{A}$ is the magnetic vector potential. Over a longer closed path $\mathcal{C}$, a Wilson loop operator $\mathcal{W}_\mathcal{C}$ is the path-ordered multiplication of $\hat{U}_{\alpha,\beta}$ along links in $\mathcal{C}$. In the confined phase, $\mathcal{W}_\mathcal{C}$ satisfies an area law $\langle\mathcal{W}_\mathcal{C}\rangle \sim e^{-\text{area}(\mathcal{C})}$. In the deconfined phase, it satisfies $\langle\mathcal{W}_\mathcal{C}\rangle \sim e^{-\text{perimeter}(\mathcal{C})}$.

A 't Hooft string operator is defined as a directed product of electric link operators $\hat{\Upsilon}(\varphi) = \prod_n \exp(i\varphi \hat{E}_{na_x, na_x+a_y})$; in Ref. [47] (Sec. IB) we show that in the QLM it acts a disorder parameter. This operator changes the value of the magnetic flux by an amount φ on the plaquettes where it starts and ends, introducing a pair of magnetic vortices. In the confining phase it is ordered, i.e., $\langle\hat{\Upsilon}(\varphi)\rangle \neq 0$ for $\varphi \neq 0$ in $2+1$ dimensions. The fact that a nonzero expectation value of the disorder parameter characterizes a confinement phase in a gauge model may simplify the signal-to-noise problem in an actual quantum simulation.

In Fig. 2(a) we show the disorder parameter $\hat{\Upsilon}$ for $\hat{H}_{\text{QLM}}$ on the quasi-2D ladder lattice, shown in Fig. 1(c), calculated using DMRG calculation. The ladder is the minimal lattice exemplifying a $2+1$ dimensional system. Clearly, $\hat{\Upsilon}$ is nonzero in the strong coupling regime $g_{\text{elec}}^2 g_{\text{mag}}^2 \gg 1$, indicative of a confining phase. Thus, even in this limited geometry, the QLM captures confinement physics. In what follows, we propose an analog QLM simulator to study ground state and dynamical phenomena on computationally challenging 2D lattices.

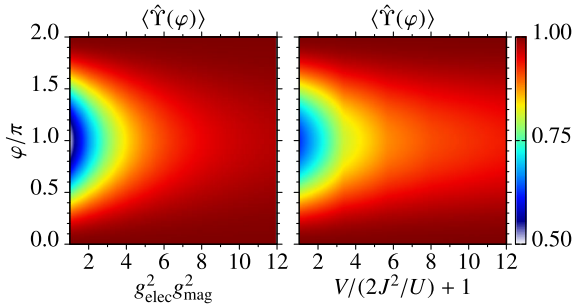

FIG. 2. Expectation value of the 't Hooft string $\hat{\Upsilon}(\varphi)$ which inserts a flux φ at the plaquette in the middle of a ladder [see Fig. 1(c)]. Left panel: value in the ground state of the pure gauge model $\hat{H}_{\text{QLM}}$ as a function of the electric coupling g_{elec}^2 with a perturbative value of the magnetic coupling $(1/g_{\text{mag}}^2) \sim (2J^2/U) \to (2/75)$. Right panel: value in the ground state of the two-body Hamiltonian $\hat{H}_{\text{imp}}$ as a function of the on-site energy V, with $J = 1$ and $U = 75$. Numerics were performed for a size $L = 29$ rung ladder with 85 spins using DMRG calculation with 300 states and a truncation error estimated at $< 10^{-12}$. From the plots, $\langle\hat{\Upsilon}\rangle \geq 0.5$ is indicative of a confining phase. The equivalence between the implemented model (3) and the gauge invariant model (4) in the strongly coupled and intermediately coupled regimes is evident.

Implementation with superconducting devices.—To simulate a $U(1)$ QLM, there are three elements: (i) the local Hilbert space, labeled by the electric flux on the lattice links; here, the Hilbert space is spanned by a discrete set of states of a fluxonium device, (ii) Gauss' law on the lattice vertices; here, this is imposed by strong interactions between devices, mediated by tunable inductive couplings, (iii) the gauge invariant dynamics; here, this emerges at second order of perturbation with capacitive couplings between neighboring devices.

We propose a lattice of fluxonium devices [51], which are inductively shunted superconducting Josephson junctions with demonstrated relaxation times on the order of 1 ms [52,53], located on the edges and vertices of the square lattice, as shown in Figs. 1(a) and 1(b). The Hamiltonian for device k is

$$\hat{H}_k = 4E_C\hat{n}_k^2 + \hat{P}(\hat{\phi}_k), \tag{2}$$

where $\hat{P}(\hat{\phi}_k) = -E_J\cos(\hat{\phi}_k + \phi_{\text{off}}) + E_L\hat{\phi}_k^2/2$ is the local potential, $E_C = e^2/(2C)$ is the charging energy of the island with total capacitance C, $E_J = (\hbar/2e)^2(1/L_J)$ is the Josephson energy with L_J the effective inductance of the Josephson junction, $E_L = (\hbar/2e)^2(1/L)$ is the shunt inductive energy, and $E_J \geq E_C > E_L$.

The phase $\hat{\phi}_k$ is proportional to the (physical) flux in the device. It is not compact, so the conjugate charge $\hat{n}_k = -i(\partial/\partial\phi_k)$ takes continuous values. The offset phase $\phi_{\text{off}} = 2\pi\Phi_{\text{ext}}/\Phi_0$, where Φ_{ext} is a tunable flux [53] and $\Phi_0 = h/(2e)$ is the flux quantum. The potential terms can be tuned to support integer representations of the electric flux by setting $\phi_{\text{off}} = 0$, shown in Fig. 3(a), or half-integer representations with $\phi_{\text{off}} = \pi$, Fig. 3(b). In the limit $E_J \sim E_C \gg E_L$, the lowest energy states are the first band Wannier functions with mean (physical) flux $\langle\hat{\phi}_k\rangle = 2\pi m_k$, and zero-point phase fluctuations $\sigma_\phi = (8E_C/E_J)^{1/4}$.

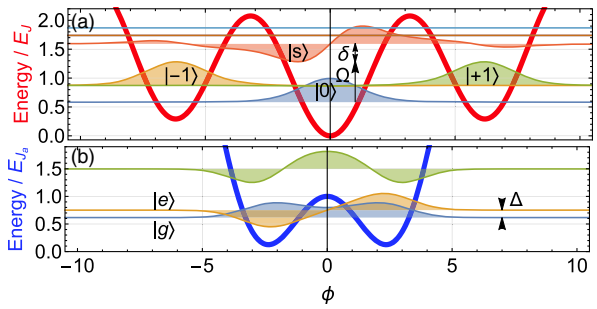

FIG. 3. (a) Link fluxonium devices operate as qutrits with $\phi_{\text{off}} = 0$. The potential $P(\phi_{\text{link}})$ (red) and the eigenfunctions are plotted for qutrit states $|0\rangle, |\pm 1\rangle$, which represent electric flux, and the next energy state $|s\rangle$. A cavity field couples states $|0\rangle \leftrightarrow |s\rangle$ with Rabi frequency Ω and detuning δ to tune the electric coupling in the QLM. (b) Ancilla fluxonium potential $P(\phi_a)$ (blue) with $\phi_{\text{off}} = \pi$, and eigenfunctions $|g\rangle$ and $|e\rangle$. Ancillae are initialized in state $|e\rangle$ and generate the Gauss constraint on link devices through an effective interaction.

The Gauss law constraint is enforced by ancillary fluxonium devices at lattice vertices, with parameters E_J^a, E_C^a, E_L^a and $\phi_{\text{off}}^a = \pi$. The lowest energy states $|g\rangle$ and $|e\rangle$ are shown in Fig. 3(b). Each ancilla is inductively coupled to its neighbors, $\hat{H}_{\text{ind}} = (E_L^c/2)\sum_v\sum_{k=1}^4(\hat{\phi}_k - \hat{\phi}_a)^2$, where $E_L^c = (\hbar/2e)^2(1/L_c)$, and L_c is the coupling inductance. Ancillae are initialized in the long-lived excited state $|e\rangle$, for which $T_1 > 1$ ms [53].

At first order in E_L^c/Δ, the interaction $\hat{H}_{\text{ind}}$ is zero since $|e\rangle$ is antisymmetric. At second order we obtain an effective Hamiltonian acting on the links around each vertex. We only include the terms diagonal in the $|m_k\rangle$ basis since the off diagonal terms are much smaller by a factor $\sim e^{-\pi^2/\sigma^2}$. The total Hamiltonian, local plus inductive interaction for a spin-S representation is then $\sum_k\hat{H}_k + \hat{H}_{\text{ind}} = V\sum_k S_k^{z2} + U\sum_v(\sum_{k\in\mathcal{N}(v)}\hat{S}_k^z)^2$, where $\hat{S}^z = \sum_{m=-S}^S m|m\rangle\langle m|$, $U = E_L^{c\,2}|\langle g|\hat{\phi}_a|e\rangle|^2|\langle\hat{\phi}\rangle_{m=1}|^2/\Delta > 0$, $\mathcal{N}(v)$ is the neighborhood of a vertex v (see Ref. [47], Sec. IIB), $\Delta = E_e - E_g > 0$ is the ancilla qubit energy splitting including local contributions from the inductive coupling, calculated using Eq. (2) with the replacement $E_L^a \to E_L^a + 4E_L^c$, and V (which generates the QLM electric coupling g_{elec}^2) is the qutrit energy splitting $E_1 - E_0$, computed using Eq. (2) with $E_L \to E_L + 2E_L^c$.

The QLM magnetic coupling g_{mag}^2 is generated by a capacitive coupling between link devices, $\hat{H}_{\text{cap}} = 8E_C^c\sum_{\langle k,j\rangle}\hat{n}_k\hat{n}_j$, where $E_C^c/E_C \simeq \{\sqrt{8+\xi^{-2}}K_0(\xi^{-1})/4\xi K[-16\xi^2/(8+\xi^{-2})]\}$, $\xi \equiv \sqrt{C_c/C}$ and C_c is the capacitance between nearest neighbors, $K_0(x)$ is a modified Bessel function, and $K(x)$ is an elliptic integral (see Ref. [47], Sec. IIC). The operators $\hat{n}$ generate displacements in phase, so the interaction drives fluctuations in the electric flux m_k. Longer range couplings decay exponentially in island separation, with a correlation length ξ. The total two body Hamiltonian is

$$\hat{H}_{\text{imp}} = V\sum_k S_k^{z2} + U\sum_v\left(\sum_{k\in\mathcal{N}(v)}\hat{S}_k^z\right)^2 + J\sum_{\langle j,k\rangle}(\hat{S}_j^+\hat{S}_k^- + \hat{S}_j^-\hat{S}_k^+) \tag{3}$$

with $J = -8E_C^c|\langle 1|\hat{n}|0\rangle|^2$. In the limit $U \gg |J|$, the second term projects the ground states into the gauge invariant subspace and the effective Hamiltonian is

$$\hat{H}_{\text{eff}} = (V + 2J^2/U)\sum_j\hat{S}_j^{z2} - (2J^2/U)\sum_{\square}(\hat{S}^+\hat{S}^-\hat{S}^+\hat{S}^- + \text{H.c.}) + (J^2/4U)\sum_{\langle j,k\rangle}\hat{S}_j^z\hat{S}_k^z(1 - \hat{S}_j^z\hat{S}_k^z). \tag{4}$$

This is the first key element of our proposal: defining $g_{\text{elec}}^2 = V + 2J^2/U$ and $1/g_{\text{mag}}^2 = 2J^2/U$, the first two

terms of $\hat{H}_{\rm eff}$ are equivalent to the gauge Hamiltonian $\hat{H}_{\rm QLM}$, Eq. (1), once we identify $\hat{E} \mapsto \hat{S}^z$ and $\hat{U} \mapsto \hat{S}^-$; notice the latter is nonunitary unlike the continuum case. The third term respects all the symmetries of the gauge invariant model, and renormalizes the electric field and U. Comparison of DMRG calculations of $\hat{H}_{\rm QLM}$ [Fig. 2(a)] and $\hat{H}_{\rm eff}$ [Fig. 2(b)] on a ladder geometry shows that $\hat{H}_{\rm eff}$ replicates the confinement physics ($\hat{\Upsilon} \neq 0$) of the original QLM. We note that higher order corrections to the gauge invariant Hamiltonian in Eq. (4) may lead to an effective coupling to matter field. In this case, the behavior of the Wilson loops and 't Hooft strings in $(2+1)$D is uncertain, and left open to further study [54].

We now discuss different limits of the model based on the three level (spin-1) $U(1)$ QLM shown in Fig. 3(a). The interaction energies are determined by diagonalizing the local fluxonium Hamiltonian and computing wavefunction overlaps (see Ref. [47], Sec. IID). We show how to prepare the strongly coupled limit, which is close to the product state $\otimes_{\rm links} |0\rangle_j$, and then reduce the coupling to the intermediate limit.

Strong coupling.—Because $\hat{H}_{\rm ind}$ contributes both to U and V in $\hat{H}_{\rm imp}$ with comparable magnitudes and $|J| \ll U$, in order to satisfy the Gauss constraint, the system will be in the strong coupling regime. To enforce this, the Josephson energy on the ancilla islands E_J^a is the biggest energy scale of the model, which determines the cascade of energies: $E_J = E_C^a = 0.2E_J^a$, $E_C = 0.06E_J^a$, $E_C^c = 0.04E_J^a$, $E_L^a = 0.01E_J^a$, $E_L = 0.003E_J^a$, and $E_L^c = 0.0002E_J^a$. The link states $|\pm 1\rangle$ are then nearly degenerate with splitting $0.0006E_J^a$ and $E_L^c/\Delta = 0.023$ ensuring that the perturbation theory on the ancilla is valid. We find $U/E_J^a = 0.006$, $V/E_J^a = 0.06$, and $J/U = -0.04$, which by Eq. (1) gives $g_{\rm elec}^2 g_{\rm magn}^2 \sim 3000$. Josephson energies $E_J = 210$ GHz [55], capacitive energies $E_C = 14.2$ GHz [56], and inductive energies $E_L = 0.52$ GHz [57] have been reported, suggesting the simulation coupling strengths here are within reach of experimentally demonstrated values.

Intermediate coupling.—To reduce the electric field term we shift the energy of state $|0\rangle$ by off-resonant coupling to an excited state $|s\rangle$, above the qutrit subspace. Consider a driving field that couples to the fluxonium at frequency ω_F, which is detuned from the $|0\rangle \to |s\rangle$ transition by $\delta = \omega_F - (E_s - E_0)$. Because of the anharmonic energy spacing of the fluxonium the frequency ω_F can be chosen to be very far off resonant for other possible transitions. Inductive coupling via a quarter wavelength transmission line gives a time dependent fluxonium-field interaction $\hat{H}_{FF} = (\Omega/2)|s\rangle\langle 0|e^{-i\omega_F t} + \text{H.c.}$, where the Rabi frequency is $\Omega = -g\langle s|\hat{\phi}|0\rangle$ and g depends on physical properties of the transmission line and fluxonium [57]. Assuming other excited states are far detuned, $\hat{H}_{\rm imp}$ in the qutrit subspace is modified by $V \to V + |\Omega|^2/(4\delta)$, so V can be reduced by choosing $\delta < 0$. There are energy shifts from off-resonant coupling to multiple excited states by all three qutrit states. Optimizing ω_F and g to minimize V gives $\omega_F = 1.588E_J$ and $|g|^2 = 0.2$, so that $g_{\rm elec}^2 g_{\rm mag}^2 \simeq 1$.

Decoherence.—Spin decoherence limits the ultimate size of the simulator. We envision starting in the gapped product state $|G(0)\rangle = \prod_{\rm links}|0\rangle$ by tuning parameters to the extremely strongly coupled regime (with $\Omega = 0$), and adiabatically evolving the ground state to an intermediate coupling regime. The adiabatic evolution could be done by slowly increasing the driving field Rabi frequency over a time $T_{\rm sim}$ and, as described below, nonlocal order parameters can be measured as a function of final coupling strength [see Fig. 2(b)]. As shown in Ref. [47] (Sec. IIIB), the ground state $|G(t)\rangle$ is gapped throughout with energy $\Delta E_{\rm gap}(t) \sim 4g_{\rm elec}^2(t)$, and from the effective model $\hat{H}_{\rm eff}$ is minimal at $V = 0$ where $\Delta E_{\rm gap}^{\rm min} \sim 8J^2/U$. The decoherence times for fluxonium tuned to the qutrit point have been reported at $T_1 \sim T_2 \sim 50$ μs [53]. Consider $U = 0.032E_J$ as above and choose $E_J = 40$ GHz and $T_{\rm sim} = 2/\Delta E_{\rm gap}^{\rm min} = 0.135$ μs. The inverted ancilla qubit lifetime is $T_1^a \sim 1$ ms [53], giving an error rate per ancilla of $1 - e^{-T_{\rm sim}/T_1^a} \sim 10^{-4}$, allowing reliable simulations on a lattice with $\sim$1000 link spins.

Nonlocal measurement.—The second key element of our proposal is the measurement of spin-1 Wilson loop operators $\mathcal{W}_\mathcal{C} = \hat{S}^+ \otimes \hat{S}^- \otimes \cdots \otimes \hat{S}^+ \otimes \hat{S}^-$ on $\mathcal{C}$, and 't Hooft disorder operators $\hat{\Upsilon}(\varphi) = e^{-i\varphi\hat{S}_0^z} \otimes e^{i\varphi\hat{S}_1^z} \otimes \cdots \otimes e^{i\varphi\hat{S}_{n-1}^z}$ on a line extending from a spin "0" on the boundary. Importantly, the measurement does not alter the observable being measured, and repeated measurements give the same result; i.e., it is nondemolition. The idea is to prepare the ground state of the spin-1 lattice Hamiltonian, turn off $\hat{H}_{\rm imp}$, and then measure $\mathcal{W}_\mathcal{C}$ or $\hat{\Upsilon}(\varphi)$. Thus, the measurement can "quench" the system, in order to study the ensuing dynamics and multitime correlations when the Hamiltonian is turned on again [58].

To measure nonlocal operators, a subset of spins in the array are coupled to a single microwave cavity mode, Fig. 1(c). Ultimately, only a single qubit degree of freedom need be measured, which is advantageous if the measurement error is significant. By contrast, if spins were measured independently the fidelity would decrease exponentially with operator size.

We require a dispersive coupling of spins in a region $\mathcal{R}$, $\hat{H}_{\rm int} = -\chi\hat{a}^\dagger\hat{a}\sum_{j\in\mathcal{R}}|0\rangle_j\langle 0|$, and a coupling between an ancilla A (such as one of the ancilla qubits) and the bosonic field, $\hat{H}_{\rm int}^A = -\chi_A\hat{a}^\dagger\hat{a}|e\rangle_A\langle e|$, where $\hat{a}^\dagger$ and $\hat{a}$ are bosonic creation and annihilation operators. Selectively addressing cavity coupling within the region $\mathcal{R}$ or at the ancilla location can be done by coherently mapping noninteracting spins to noninteracting local states, which are far detuned from the cavity coupling. In Ref. [47] (Sec. III) we describe

in detail two methods to measure $\mathcal{W}_\mathcal{C}$ or $\hat{\Upsilon}(\varphi)$. In brief, one method uses a geometric phase gate, requiring only the ability to prepare the vacuum state of the cavity and a sequence of displacement operators and evolution generated by $\hat{H}_{\rm int}$. An alternative method can be done in a single step but requires the preparation of a superposition of vacuum and a single photon state of the cavity.

Fidelity.—To estimate process fidelity, we assume the cavity has a decay rate κ, and system and ancilla spins depolarize independently with an error rate γ. On n spins, the geometric phase-gate measurement process fidelity is

$$F_{\rm pro}^{(gp)}(\theta,\Omega) > \eta_A[1-n(4\pi+6\theta)\gamma/|\chi|] \times [1-\pi\Omega\kappa(e^{-3\theta\kappa/|\chi|}+e^{-\theta\kappa/|\chi|})(1+\pi\kappa/2|\chi|)/|\chi|], \quad (5)$$

where $\eta_A < 1$ describes the finite detection fidelity of the ancilla spin. For measuring Wilson loops $\Omega = \pi/\sqrt{3}$, $\theta = 2\pi/3$, while for measuring 't Hooft strings $\Omega = \pi/2$, $\theta = \pi/2$. For the single photon implementation, the process fidelity is $F_{\rm pro}^{(sp)}(\theta) > \eta_p[1-n(1-e^{-\gamma\bar{t}(\theta)})]$, where $\eta_p \leq 1$ describes finite single photon detection fidelity, and the mean gate time is $\bar{t}(\theta) = [(1+e^{2\theta\kappa/|\chi|})(2\theta)^2\kappa/|\chi|^2]/(2\theta\kappa/|\chi| + e^{2\theta\kappa/|\chi|} - 1)$. In the presence of inhomogeneities in the dispersive coupling strength χ, the error $\mathcal{E}$ for the global gates with angle θ is $\mathcal{E} \approx \theta^2|\mathcal{R}|(|\mathcal{R}|-1)\epsilon^2/2$, where ϵ is the fractional cavity mode field variation across the lattice (Ref. [47], Sec. IIIA).

Using transmons coupled to a 3D microwave cavity [60] the following values were reported for one island: $\gamma =$ 66.7 kHz, $|\chi|/2\pi = 99.8$ MHz, $\kappa = 22.2$ kHz. Single-shot transmon qubit measurements have also been reported with $\eta_A = 0.919$ [61]. With efficient single microwave photon detectors, the single photon protocol allows for a measurement of a Wilson loop on $n-1$ spins with fidelity $F_{\rm pro}^{(sp)} > \eta_p(1-2.5\times10^{-3}n)$. Microwave photon number resolution can be achieved with $\eta_p \simeq 0.90$ [62,63]. Assuming similar parameters for fluxonium and local addressability, using either the geometric phase gate or the single photon gate, a Wilson loop of length 8 or a 't Hooft string of size 10 could be measured with ~90% fidelity. By the nondestructive nature of the measurement, the imperfect detection efficiency can be improved by repeating the measurement until the presence or absence of a photon is known with high confidence, enabling measurement of much larger loops.

In summary, we provide a proposal for an analog $2+1$D QLM simulator using a 2D array of superconducting devices. The simulator can be tuned between intermediate and strong coupling regimes, and allows nondestructive measurement of nonlocal, spacelike QLM order and disorder parameters, resolving an outstanding gap in other proposals. Moreover, we provide a physical encoding of the states for the QLM, where local electric field terms are nontrivial. The protocol is rather robust to inhomogeneities, allowing for implementations in superconducting arrays, and we have presented numerical evidence that lattice QED in "quasi-2" + 1 dimensions exhibits confinement. Beyond ground state characterization, the simulator can be used to probe dynamics and measure the evolution of nonlocal order or disorder parameters.

This work was partially supported by the ARC Centre of Excellence for Engineered Quantum Systems EQUS (Grant No. CE110001013). We also acknowledge financial support from Basque Government Grants IT472-10, Spanish MINECO FIS2012-36673-C03-02, UPV/EHU Project No. EHUA15/17, UPV/EHU UFI 11/55 and the SCALEQIT EU project. G. P. and D. V. acknowledge support by the ERC-St Grant ColdSIM (No. 307688), EOARD, UdS via Labex NIE and IdEX, RYSQ.

[1] K. G. Wilson, Confinement of quarks, Phys. Rev. D **10**, 2445 (1974).
[2] H. J. Rothe, *Lattice Gauge Theories* (World Scientific, Singapore, 2012).
[3] X. G. Wen, *Quantum Field Theory of Many-Body Systems: From the Origin of Sound to an Origin of Light and Electrons*, Oxford Graduate Texts (Oxford University Press, New York, 2004).
[4] G. 't Hooft, On the phase transition towards permanent quark confinement, Nucl. Phys. **B138**, 1 (1978).
[5] D. Horn, Finite matrix models with continuous local gauge invariance, Phys. Lett. **100B**, 149 (1981).
[6] P. Orland and D. Rohrlich, Lattice gauge magnets: Local isospin from spin, Nucl. Phys. **B338**, 647 (1990).
[7] S. Chandrasekharan and U-J. Wiese, Quantum link models: A discrete approach to gauge theories, Nucl. Phys. **B492**, 455 (1997).
[8] D. S. Rokhsar and S. A. Kivelson, Superconductivity and the quantum hard-core dimer gas, Phys. Rev. Lett. **61**, 2376 (1988).
[9] A. M. Polyakov, *Gauge Fields and Strings* (Harwood Academic Publishers, London, 1987).
[10] *Lattice QCD for Nuclear Physics*, edited by H.-W. Lin and H. B. Meyer (Springer, Heidelberg, 2015).
[11] T. Byrnes, P. Sriganesh, R. J. Bursill, and C. J. Hamer, Density matrix renormalisation group approach to the massive Schwinger model, Phys. Rev. D **66**, 013002 (2002).
[12] M. C. Banuls, K. Cichy, K. Jansen, and J. I. Cirac, The mass spectrum of the Schwinger model with matrix product states, J. High Energy Phys. 11 (2013) 158.
[13] M. C. Banuls, K. Cichy, J. I. Cirac, K. Jansen, and H. Saito, Matrix product states for lattice field theories, PoS, LATTICE 2013, **332** (2013).
[14] E. Rico, T. Pichler, M. Dalmonte, P. Zoller, and S. Montangero, Tensor Networks for Lattice Gauge Theories and Atomic Quantum Simulation, Phys. Rev. Lett. **112**, 201601 (2014).

[15] B. Buyens, J. Haegeman, K. Van Acoleyen, H. Verschelde, and F. Verstraete, Matrix product states for gauge field theories, Phys. Rev. Lett. **113**, 091601 (2014).
[16] P. Silvi, E. Rico, T. Calarco, and S. Montangero, Lattice gauge tensor networks, New J. Phys. **16**, 103015 (2014).
[17] L. Tagliacozzo, A. Celi, and M. Lewenstein, Tensor networks for lattice gauge theories with continuous groups, Phys. Rev. X **4**, 041024 (2014).
[18] T. Pichler, M. Dalmonte, E. Rico, P. Zoller, and S. Montangero, Real-time dynamics in U(1) lattice gauge theories with tensor networks, Phys. Rev. X **6**, 011023 (2016).
[19] B. Buyens, J. Haegeman, H. Verschelde, and F. Verstraete, and K. Van Acoleyen, Confinement and string breaking for QED2 in the Hamiltonian picture, arXiv:1509.00246.
[20] J. Haegeman, K. Van Acoleyen, N. Schuch, J. I. Cirac, and F. Verstraete, Gauging quantum states: From global to local symmetries in many-body systems, Phys. Rev. X **5**, 011024 (2015).
[21] S. Kuhn, E. Zohar, J. I. Cirac, and M. C. Banuls, Non-Abelian string breaking phenomena with matrix product states, J. High Energy Phys. 07 (2015) 130.
[22] E. Zohar, M. Burrello, T. B. Wahl, and J. I. Cirac, Fermionic projected entangled pair states and local U(1) gauge theories, Ann. Phys. (Amsterdam) **363**, 385 (2015).
[23] E. Zohar and M. Burrello, Building projected entangled pair states with a local gauge symmetry, New J. Phys. **18**, 043008 (2016).
[24] H. Weimer, M. Muller, I. Lesanovsky, P. Zoller, and H. P. Büchler, A Rydberg quantum simulator, Nat. Phys. **6**, 382 (2010).
[25] L. Tagliacozzo, A. Celi, A. Zamora, and M. Lewenstein, Optical Abelian lattice gauge theories, Ann. Phys. (Amsterdam) **330**, 160 (2013).
[26] A. W. Glaetzle, M. Dalmonte, R. Nath, I. Rousochatzakis, R. Moessner, and P. Zoller, Quantum spin-ice and dimer models with Rydberg atoms, Phys. Rev. X **4**, 041037 (2014).
[27] E. Kapit and E. Mueller, Optical-lattice Hamiltonians for relativistic quantum electrodynamics, Phys. Rev. A **83**, 033625 (2011).
[28] E. Zohar and B. Reznik, Confinement and lattice quantum-electrodynamic electric flux tubes simulated with ultra-cold atoms, Phys. Rev. Lett. **107**, 275301 (2011).
[29] J. Casanova, L. Lamata, I. L. Egusquiza, R. Gerritsma, C. F. Roos, J. J. Garcia-Ripoll, and E. Solano, Quantum simulation of quantum field theories in trapped ions, Phys. Rev. Lett. **107**, 260501 (2011).
[30] E. Zohar, J. I. Cirac, and B. Reznik, Simulating compact quantum electrodynamics with ultra-cold atoms: Probing confinement and non-perturbative effects, Phys. Rev. Lett. **109**, 125302 (2012).
[31] D. Banerjee, M. Dalmonte, M. Muller, E. Rico, P. Stebler, U.-J. Wiese, and P. Zoller, Atomic quantum simulation of dynamical gauge fields coupled to fermionic matter: From string breaking to evolution after a quench, Phys. Rev. Lett. **109**, 175302 (2012).
[32] E. Zohar, J. I. Cirac, and B. Reznik, Simulating $(2+1)$-dimensional lattice QED with dynamical matter using ultracold atoms, Phys. Rev. Lett. **110**, 055302 (2013).
[33] P. Hauke, D. Marcos, M. Dalmonte, and P. Zoller, Quantum simulation of a lattice Schwinger model in a chain of trapped ions, Phys. Rev. X **3**, 041018 (2013).
[34] E. Zohar, J. I. Cirac, and B. Reznik, Quantum simulations of gauge theories with ultra-cold atoms: Local gauge invariance from angular-momentum conservation, Phys. Rev. A **88**, 023617 (2013).
[35] K. Stannigel, P. Hauke, D. Marcos, M. Hafezi, S. Diehl, M. Dalmonte, and P. Zoller, Constrained dynamics via the Zeno effect in quantum simulation: Implementing non-Abelian lattice gauge theories with cold atoms, Phys. Rev. Lett. **112**, 120406 (2014).
[36] S. Notarnicola, E. Ercolessi, P. Facchi, G. Marmo, S. Pascazio, and F. V. Pepe, Discrete Abelian gauge theories for quantum simulations of QED, J. Phys. A: Math. Theor. **48**, 30FT01 (2015).
[37] A. Bazavov, Y. Meurice, S.-W. Tsai, J. Unmuth-Yockey, and J. Zhang, Gauge-invariant implementation of the Abelian Higgs model on optical lattices, Phys. Rev. D **92**, 076003 (2015).
[38] A. Bermudez and D. Porras, Interaction-dependent photon-assisted tunneling in optical lattices: A quantum simulator of strongly correlated electrons and dynamical gauge fields, New J. Phys. **17**, 103021 (2015).
[39] U.-J. Wiese, Towards quantum simulating QCD, Nucl. Phys. **A931**, 246 (2014).
[40] E. Zohar, J. I. Cirac, and B. Reznik, Quantum simulations of lattice gauge theories using ultra-cold atoms in optical lattices, Rep. Prog. Phys. **79**, 014401 (2016).
[41] D. Marcos, P. Rabl, E. Rico, and P. Zoller, Superconducting circuits for quantum simulation of dynamical gauge fields, Phys. Rev. Lett. **111**, 110504 (2013).
[42] D. Marcos, P. Widmer, E. Rico, M. Hafezi, P. Rabl, U.-J. Wiese, and P. Zoller, Two-dimensional lattice gauge theories with superconducting quantum circuits, Ann. Phys. (Amsterdam) **351**, 634 (2014).
[43] L. Garcia-Alvarez, J. Casanova, A. Mezzacapo, I. L. Egusquiza, L. Lamata, G. Romero, and E. Solano, Fermion-fermion scattering in quantum field theory with superconducting circuits, Phys. Rev. Lett. **114**, 070502 (2015).
[44] A. Mezzacapo, E. Rico, C. Sabin, I. L. Egusquiza, L. Lamata, and E. Solano, Non-Abelian lattice gauge theories in superconducting circuits, Phys. Rev. Lett. **115**, 240502 (2015).
[45] J. Kogut and L. Susskind, Hamiltonian formulation of Wilsons lattice gauge theories, Phys. Rev. D **11**, 395 (1975).
[46] V. E. Manucharyan, J. Koch, L. I. Glazman, and M. H. Devoret, Fluxonium: Single cooper-pair circuit free of charge offsets, Science **326**, 113 (2009).
[47] See Supplemental Material at http://link.aps.org/supplemental/10.1103/PhysRevLett.117.240504 for analysis on: large-N representation and duality transformation, the implementation with fluxonia, measurement of non-local order parameters, and gauge invariance and "dressed" quantum states, which includes Ref. [48–50].
[48] A. M. Rey, G. Pupillo, C. W. Clark, and C. J. Williams, Ultra-cold atoms confined in an optical lattice plus parabolic potential: A closed-form approach, Phys. Rev. A **72**, 033616 (2005).

[49] L. Jiang, G. K. Brennen, A. V. Gorshkov, K. Hammerer, M. Hafezi, E. Demler, M. D. Lukin, and P. Zoller, Anyonic interferometry and protected memories in atomic spin lattices, Nat. Phys. **4**, 482 (2008).

[50] G. K. Brennen, K. Hammerer, L. Jiang, M. D. Lukin, and P. Zoller, Global operations for protected quantum memories in atomic spin lattices, arXiv:0901.3920.

[51] S. M. Girvin, Circuit QED: superconducting qubits coupled to microwave photons, in *Quantum Machines: Measurement and Control of Engineered Quantum Systems*, Lecture Notes of the Les Houches Summer School Vol. 96, edited by M. Devoret, B. Huard, R. Schoelkopf, and L. F. Cugliandolo (Oxford University Press, Oxford, 2011).

[52] U. Vool, I. M. Pop, K. Sliwa, B. Abdo, C. Wang, T. Brecht, Y. Y. Gao, S. Shankar, M. Hatridge, G. Catelani, M. Mirrahimi, L. Frunzio, R. J. Schoelkopf, L. I. Glazman, and M. H. Devoret, Non-Poissonian quantum jumps of a Fluxonium qubit due to quasiparticle excitations, Phys. Rev. Lett. **113**, 247001 (2014).

[53] I. M. Pop, K. Geerlings, G. Catelani, R. J. Schoelkopf, L. I. Glazman, and M. H. Devoret, Coherent suppression of electromagnetic dissipation due to superconducting quasiparticles, Nature (London) **508**, 369 (2014).

[54] E. Fradkin, *Field Theories of Condensed Matter Physics*, 2nd ed. (Cambridge University Press, Cambridge, England, 2013).

[55] J. Bylander, S. Gustavsson, F. Yan, F. Yoshihara, K. Harrabi, G. Fitch, D. G. Cory, Y. Nakamura, J.-S. Tsai, and W. D. Oliver, Noise spectroscopy through dynamical decoupling with a superconducting flux qubit, Nat. Phys. **7**, 565 (2011).

[56] D. Vion, A. Aassime, A. Cottet, P. Joyez, H. Pothier, C. Urbina, D. Esteve, and M. H. Devoret, Manipulating the quantum state of an electrical circuit, Science **296**, 886 (2002).

[57] N. A. Masluk, Ph.D. thesis, Yale University, 2012.

[58] It was proven in Ref. [59] that nondemolition measurements of spacelike non-Abelian Wilson loops are not physical because they would allow for faster than light signaling. However, Abelian Wilson loops such as considered here have no such obstruction provided the spins on the loop have access to a shared entanglement resource, which here is the common cavity mode.

[59] D. Beckman, D. Gottesman, A. Kitaev, and J. Preskill, Measurability of Wilson loop operators, Phys. Rev. D **65**, 065022 (2002).

[60] H. Paik, D. I. Schuster, L. S. Bishop, G. Kirchmair, G. Catelani, A. P. Sears, B. R. Johnson, M. J. Reagor, L. Frunzio, L. I. Glazman, S. M. Girvin, M. H. Devoret, and R. J. Schoelkopf, Observation of high coherence in Josephson junction qubits measured in a three-dimensional circuit QED architecture, Phys. Rev. Lett. **107**, 240501 (2011).

[61] Y. Liu, S. Srinivasan, D. Hover, S. Zhu, R. McDermott, and A. A. Houck, High fidelity single-shot readout of a transmon qubit using a SLUG micro-wave amplifier, New J. Phys. **16**, 113008 (2014).

[62] B. R. Johnson, M. D. Reed, A. A. Houck, D. I. Schuster, L. S. Bishop, E. Ginossar, J. M. Gambetta, L. DiCarlo, L. Frunzio, S. M. Girvin, and R. J. Schoelkopf, Quantum nondemolition detection of single microwave photons in a circuit, Nat. Phys. **6**, 663 (2010).

[63] S. R. Sathyamoorthy, L. Tornberg, A. F. Kockum, B. Q. Baragiola, J. Combes, C. M. Wilson, T. M. Stace, and G. Johansson, Quantum non-demolition detection of a propagating microwave photon, Phys. Rev. Lett. **112**, 093601 (2014).